Concurrent Geometric Distortion Correction in Mapping Slice-to-volume (MSV) Motion Correction of fMRI Time Series

D. Yeo[1,2], J. A. Fessler[1,2], B. Kim[2]

[1]Electrical Engineering and Computer Science, University of Michigan, Ann Arbor, MI, United States, [2]Radiology, University of Michigan Medical School, Ann Arbor, MI, United States

Introduction: The accuracy of measuring voxel intensity changes between stimulus and rest images in fMRI echo-planar imaging (EPI) data, from which brain activation maps are computed, is severely degraded in the presence of rigid head motion. In addition, EPI is sensitive to susceptibility-induced geometric distortions, especially in the mid to lower brain images. Head motion causes image shifts as well as field-map changes which result in local changes in geometric distortion. Commonly, geometric distortion correction is performed, with a static field-map, independently of image registration. This does not account for field-map changes with head motion. Previously, the concept of a concurrent motion and field-inhomogeneity correction technique using quadratic penalized least squares (QPLS) reconstruction has been introduced as an enhancement to the map slice-to-volume (MSV) motion correction scheme that accounts for inter-slice motion [1-3]. This work is an extension of [1] and evaluates the technique under more realistic simulation conditions on an entire simulated 130-volume EPI time-series.

Theory: In EPI, field-inhomogeneity (ΔB) causes pixels to shift in the phase-encode (PE) direction y by $\gamma \Delta B(x,y) T_{readout}$ pixels where $T_{readout}$ is the readout time [4]. The QPLS reconstruction method [2] is used for geometric distortion correction while the MSV method [3], which allows each slice to have its own six DOF rigid-body transform, is used for motion correction. MSV registers EPI slices into an anatomical volume using the Nelder-Mead optimization method to find the transformation that gives the lowest mutual information metric. The concurrent correction scheme has N cycles, each of which consists of a QPLS stage followed by a MSV stage. For each slice in each cycle, the EPI system-object matrix $\mathbf{A}_l$ is computed with the current field-map $\Delta\omega_l^{(n)}$ estimated using MSV motion parameters. The object is estimated from k-space data u_l (Step 1) by minimizing a QPLS cost function via the conjugate gradient algorithm. $\mathbf{R}$ is the product of two difference matrices and β is a regularization parameter. Each slice is registered via MSV to a 3D anatomical reference to obtain motion parameters (Step 2) which are median-filtered and applied to $\Delta\omega^{(0)}$ (Step 3). The resultant volume is re-sampled to obtain new field-maps. The algorithm repeats until changes in the MSV estimates are below a threshold value. Since field-map errors may cause a larger MSV error in the PE direction, and since out-of-plane rotations may change the field-map significantly, the initial MSV estimates of t_y, θ_x and θ_y are not reliable for updating the field-map. Thus, for n=0, only t_x, t_z and θ_z are used to update the field-map. In subsequent cycles, all six DOFs are used.

***Algorithm**. Concurrent QPLS-MSV for EPI Motion Correction*

Initial data: $\Delta\omega_l^{(0)}$ *(static field-map),* u_l *(k-space data),* $l=1...L$

for $n=0...N$ *(correction cycles)*

Step 1: $\hat{f}_{l,QPLS} = \arg\min_f \frac{1}{2}\|u_l - A_l f\|^2 + \frac{\beta}{2} f^T R f$ *for* $l=1...L$ ***(QPLS)***

Use $\Delta\omega_l^{(n)}$ *to compute* A_l *above.*

Step 2: $\hat{\theta}_{l,MSV} = \arg\min_\theta \{-MI(f_l(T_\theta(r)), g_{ref}(r))\}$ *for* $l=1...L$ ***(MSV)***

Step 3: $\Delta\omega_l^{(n+1)} = \{\Delta\omega^{(0)}(T_{\hat{\theta}_{l,MSV}}(\boldsymbol{r}))\}_l$ *for* $l=1...L$ ***(resample slice l)***

end

Table 1. RMSE of MSV estimates for simulated EPI time-series

Dataset	RMSE (mm and °)					
	t_x	t_y	t_z	θ_x	θ_y	θ_z
Distorted	1.07	7.81	0.17	0.31	0.31	0.35
Cycle 0	**0.62**	**3.11**	**0.19**	**0.13**	**0.12**	**0.26**
Cycle 1	**0.76**	**0.38**	**0.22**	**0.03**	**0.04**	**0.13**
Cycle 2	**0.76**	**0.36**	**0.19**	**0.03**	**0.04**	**0.11**
Cycle 3	**0.77**	**0.37**	**0.20**	**0.03**	**0.04**	**0.11**

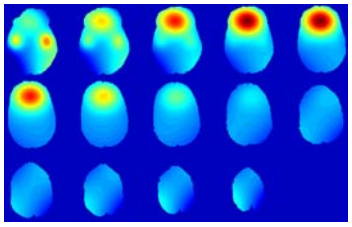

Figure 1. Simulated field-map

Methods: Two perfectly registered T_1- and T_2-weighted image datasets (matrix size: 256×256×181, voxel size: 1mm^3) from the International Consortium of Brain Mapping are used to test the concurrent correction method. Three 3D Gaussian blobs were added to a 3D third order polynomial to simulate a brain field-map (Fig. 1) which can be scaled to any desired field-inhomogeneity level. Translational and in-plane rotational motion (ground truth t_x, t_y, t_z and θ_z) were then applied to the T_2-w *and* simulated field-map volumes and sequential 5mm thick slices were re-sampled to form 130 14-slice volumes. The applied motion is smooth with respect to time and had maximum values of 7.20mm, 8.00mm, 3.51mm and 4.70° for t_x, t_y, t_z and θ_z, respectively. The T_2-w volumes obtained serve as the time-series image ground truth. The applied motion does not change the orientation of the air-tissue interface with respect to B_0 and thus is unlikely to change the field-map significantly except for the respective translation or in-plane rotation. Thus, forward distorting the T_2-w volume with the rotated-translated field-map is reasonable as long as out-of-plane rotations θ_x and θ_y are not applied. The field-map was simulated at 5 ppm at 1.5T. To forward distort the T_2-w images, the k-space data of the distorted images was first generated with the simulated field-map. The readout time was 43.8ms with a pixel bandwidth of 22.8 Hz in the PE direction. The distorted images were then reconstructed from this k-space data using a system-object matrix with the field-map set to zero.

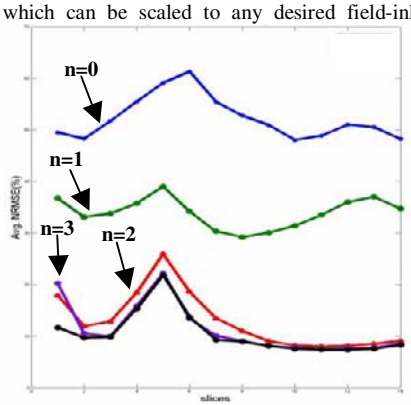

Figure 2. Average NRMSE of various cycles

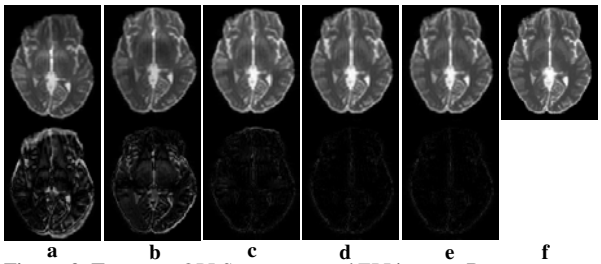

a **b** **c** **d** **e** **f**

Figure 3. **Top row:** QPLS reconstructed EPI images, **Bottom rows**: Error images. (**a**) Distorted 5ppm, (**b**) cycle 0(n=0), (**c**) cycle 1(n=1), (**d**) cycle 2(n=2), (**e**) cycle 3(n=3), (**f**) ground truth. (scale: 0 to 1)

Results: Table 1 shows that the RMSE values of the estimated MSV parameters decrease as n increases and empirically converge. The standard deviation values also behave similarly. To measure image quality, Fig. 2 shows that the normalized RMSE of each slice in the T_2-w volume averaged across time decreases as n increases. Fig. 3 shows reconstructed EPI slices from the same position in the head and their corresponding error images compared to the ground truth (Fig. 3(f)) as n increases.

Discussion: The decreasing MSV RMSE and image NRMSE values as n increases (Table 1 and Fig. 2) demonstrate the effective correction of motion artifacts that are complicated by the field effects induced by rigid head motion. In Table 1, the RMSE values remain relatively constant for n≥2 which indicate that the procedure can be terminated earlier, thus reducing the computation time. Results from another simulated dataset also show that convergence is reached at n=2. For other datasets without ground truths, the algorithm can be tasked to automatically terminate when the motion parameters' RMS differences for the last two cycles are below a threshold value. Future work will study how much out-of-plane motion, which causes local changes to the field-map, can be tolerated by the method.

Acknowledgements: This research is supported in part by NIH grants 1P01 CA87634 & R01 EB00309.

References: [1] Yeo DTB, et al, Lecture Notes in Computer Science, 2004;3217:752-760; [2] Sutton BP, et al, IEEE TMI, 2003;22:178-188; [3] Kim B, et al, MRM, 1999;41:964-972; [4] Jezzard P, et al, MRM, 1995;34:65-73